



Adsorptive desulfurization of bioethanol using activated carbon loaded with zinc oxide

Jintawat Chaichanawong, Takuji Yamamoto*, Takao Ohmori, Akira Endo

Research Institute for Innovation in Sustainable Chemistry, National Institute of Advanced Industrial Science and Technology (AIST),
1-1-1 Higashi, Tsukuba, Ibaraki 305-8565, Japan

ARTICLE INFO

Article history:

Received 30 July 2010

Received in revised form

16 September 2010

Accepted 16 September 2010

Keywords:

Adsorptive desulfurization

Bioethanol

Dimethylsulfide

Adsorption isotherm

Breakthrough curve

Activated carbon

ABSTRACT

Adsorptive desulfurization of a model bioethanol that contained dimethylsulfide (DMS) as a sulfur impurity was investigated using an activated carbon loaded with zinc oxide. We studied the effect of the amount of zinc oxide loaded on the activated carbon as well as the effect of the other impurities, such as water, acetic acid and formic acid, on liquid-phase adsorption isotherms of DMS. The amount of adsorbed DMS on the activated carbon loaded with 10 wt.% of zinc oxide doubled as compared with the virgin activated carbon. It was also revealed that the amount of DMS adsorbed on the zinc-modified activated carbon was almost unchanged by the presence of the other impurities. Dynamic adsorption performance of the activated carbon was evaluated by the measurement of a packed-bed breakthrough curve (BTC). The measured BTC was fitted by a calculated BTC based on a numerical method to estimate the mass transfer parameters in the liquid-phase desulfurization process.

© 2010 Elsevier B.V. All rights reserved.

1. Introduction

With the progress of global warming as well as exhaustion of fossil fuel, bioethanol has strongly been expected as a renewable chemical source. Production of olefin from bioethanol by the ethanol-to-olefin (ETO) conversion has recently been attempted as an alternative way of the production of olefin from petroleum [1,2]. Since bioethanol usually contains various impurities such as water and organic acids [3], purification of bioethanol has been regarded as an important issue to be solved for using bioethanol as the alternative chemical source. Depending on a species of biomass and its fermentation route, bioethanol contains a sulfur impurity, such as dimethylsulfide (DMS) [4], that influences on the catalytic reaction [5]. Yokota and Fujimoto [6] studied the effect of sulfur impurities on methanol-to-gasoline (MTG) conversion over zeolite catalyst (ZSM-5) and reported that the olefin/paraffin selectivity in the MTG reaction was influenced by the presence of the sulfur impurities. Katoh et al. [7] studied the conditions of ETO reaction over HZSM-5 catalyst, and indicated that the olefin/paraffin selectivity in the ETO reaction was also influenced by the trace amount of sulfur impurities contained in bioethanol. Therefore, desulfurization of bioethanol should be investigated for production of olefin.

Catalytic hydrodesulfurization has widely been applied to remove organic sulfur compounds, such as thiophene, thiol, sulfide and disulfide from fossil fuel [8]. To achieve deep desulfurization level, hydrodesulfurization requires a large reactor, high temperature, high pressure and a lot of hydrogen, that leads to the increase of process cost. However, for commercialization of olefin that is produced from bioethanol, purification cost of bioethanol must be reduced. Adsorption is believed to be a more economical method than catalytic hydrodesulfurization [9–11]. Activated carbon or zeolite has been applied to gas-phase adsorptive desulfurization of city gas or natural gas, that contained DMS, hydrogen sulfide and 2-methyl-2-propanethiol [12–15]. To improve adsorption capacity of activated carbon for sulfur compounds, modification with loading metal was confirmed to be effective [13]. Cui et al. [14,15] examined adsorptive desulfurization of natural gas using activated carbon loaded with FeCl_3 . The enhanced adsorption of a sulfur compound having a lone pair in the molecule on FeCl_3 can be explained in terms of Lewis acid/base interaction. The interaction is expected if a metal species loaded on activated carbon is in the oxidized form. Zinc oxide is also one of the most practical metal species for adsorptive desulfurization because of its large interaction with sulfur impurities [16]. Wang et al. [17] reported that zinc oxide nanoparticles loaded on mesoporous silica showed high H_2S adsorption capacity.

The purpose of the present study is adsorptive desulfurization of bioethanol that contains DMS as a sulfur impurity. First, we measure liquid-phase adsorption isotherms of DMS in a model ethanol

* Corresponding author. Tel.: +81 29 861 7896; fax: +81 29 861 4660.
E-mail address: yamamoto-t@aist.go.jp (T. Yamamoto).

Nomenclature

a	particle surface area per unit volume of bed [m^{-1}]
a_{mes}	specific surface area of mesopores of solid [$\text{m}^2 \text{g}^{-1}$]
a_{mic}	specific surface area of micropores of solid [$\text{m}^2 \text{g}^{-1}$]
a_{total}	total specific surface area of solid [$\text{m}^2 \text{g}^{-1}$]
c	bulk concentration of solute [kg m^{-3}]
c_0	initial concentration of solute in bulk phase [kg m^{-3}]
c_i	liquid-side concentration of solute on surface of solid [kg m^{-3}]
c_s	concentration of solute in solid [kg m^{-3}]
D_{AB}	bulk diffusion coefficient of solute [$\text{m}^2 \text{s}^{-1}$]
D_L	longitudinal diffusion coefficient [$\text{m}^2 \text{s}^{-1}$]
D_s	effective diffusion coefficient of solute in solid [$\text{m}^2 \text{s}^{-1}$]
F	flow rate of ethanol to a packed-bed [$\text{cm}^3 \text{min}^{-1}$]
k_f	liquid film mass-transfer coefficient [m s^{-1}]
k_s	mass-transfer coefficient in particle [m s^{-1}]
K_F	parameter in the Freundlich equation [$\text{mg g}^{-1} \text{ppm}^{(-1/n)}$]
n	parameter in the Freundlich equation
q	concentration of solute adsorbed on solid [mg g^{-1}]
\bar{q}	mean concentration of solute adsorbed on solid [mg g^{-1}]
q_i	solid-side concentration of solute on surface of solid [mg g^{-1}]
Re	Reynolds number
r_p	pore radius of solid [nm]
r_s	radius of solid particle [m]
Sc	Schmidt number
t	time [s]
t_b	breakthrough time [min]
T	temperature [K]
V_A	molar volume of solute [$\text{m}^3 \text{mol}^{-1}$]
V_B	molar volume of solvent [$\text{m}^3 \text{mol}^{-1}$]
V_p	pore volume of solid [$\text{cm}^3 \text{g}^{-1}$]
V_{mes}	volume of mesopores of solid [$\text{cm}^3 \text{g}^{-1}$]
V_{mic}	volume of micropores of solid [$\text{cm}^3 \text{g}^{-1}$]
V_s	superficial velocity of liquid [m s^{-1}]
V_{total}	total pore volume of solid [$\text{cm}^3 \text{g}^{-1}$]
w	weight of adsorbent packed in column [g]
z	distance along bed [m]

Greek letters

ε	void fraction of solid particle
μ	viscosity of liquid [Pa s]
ρ_b	bulk density of solid particle [kg m^{-3}]
ρ_f	density of liquid [kg m^{-3}]
ρ_s	skeletal density of solid particle [kg m^{-3}]

to study the effect of the amount of zinc oxide loaded on the activated carbon on the amount of adsorbed DMS. Then, a packed-bed breakthrough curve (BTC), that shows a transient change in concentration of DMS at the exit of a column packed with the adsorbent,

is measured to evaluate dynamic adsorption characteristics of the adsorbents. The measured BTC is analyzed based on a numerical method and the mass transfer parameters in the liquid-phase adsorptive desulfurization process are estimated. Finally, based on the parameters, a BTC under the different initial concentrations of DMS is calculated and the performance of the adsorption process for removing DMS from real bioethanol is discussed.

2. Materials and methods

2.1. Preparation of adsorbents

Commercial activated carbon (AC) in a powder form (average particle size: 185 μm) and zinc acetate ($\text{Zn}(\text{CH}_3\text{COO})_2$) were supplied from Wako Pure Chemical Industries, Ltd., Japan. The AC was modified with zinc oxide in the following manner. First, the AC was immersed in an aqueous solution of zinc acetate, and then the solution was agitated using a magnetic stirrer at the stirring speed of 200 rpm for 1 h. Next, the AC in the aqueous solution was treated with ultrasound in an ultrasonic bath (Branson 2210J 47 kHz, Emerton-Japan) for degassing, followed by filtration and drying at 323 K in a rotary evaporator. The resulted AC was heated and zinc acetate on the carbon would be decomposed at 773 K in a nitrogen gas flow for 4 h and was finally oxidized at 473 K in an air flow for 2 h. We confirmed that zinc loaded on AC was oxidized by the above treatment (Supporting information S1 is available). Thus prepared AC loaded with zinc oxide of 1 wt.% was labeled as, for example, 1% ZnO/AC. The loading ratio of ZnO on AC was determined by the thermogravimetric analysis. Since the porosity of AC significantly decreased if the loading ratio of zinc oxide was larger than 10 wt.%, we determined the maximum loading ratio as 10 wt.%. To examine the effect of pore-size distribution, a carbon cryogel (CC) [18] that possesses larger mesopores than the activated carbon was also used as an adsorbent. CC can be synthesized by the sol-gel polycondensation of, for example, resorcinol with formaldehyde, followed by freeze-drying and carbonization in an inert atmosphere. The porous properties of CC are summarized in Table 1. The material cost of CC is much higher than that of AC [19].

2.2. Determination of porous properties

Adsorption and desorption isotherms of nitrogen were measured at 77 K using an automatic gas adsorption and desorption apparatus (BEL mini, BEL Japan Inc.). All samples were degassed at 523 K under vacuum for 4 h prior to the measurement. The isotherms were analyzed by the α_s -analysis [20] to determine the porous properties.

2.3. Liquid-phase adsorption experiment

0.1 g of the prepared adsorbent was added to 40 cm^3 of a model bioethanol that contained DMS with/without the other impurities. The initial concentration of DMS was varied in the range of 0.625–10 ppm. The solution was then sealed in a capped vial and kept in a water bath at 293 K for 24 h. The vials were shaken in the

Table 1
Porous properties of activated carbon.

Adsorbent	Loading amount [wt.%]	Specific surface area			Pore volume		
		a_{total} [$\text{m}^2 \text{g}^{-1}$]	a_{mes} [$\text{m}^2 \text{g}^{-1}$]	a_{mic} [$\text{m}^2 \text{g}^{-1}$]	V_{total} [$\text{cm}^3 \text{g}^{-1}$]	V_{mes} [$\text{cm}^3 \text{g}^{-1}$]	V_{mic} [$\text{cm}^3 \text{g}^{-1}$]
AC (no ZnO)	–	1391	1023	368	1.26	1.09	0.17
1% ZnO/AC	1	1331	933	398	1.19	1.01	0.18
5% ZnO/AC	5	1265	889	376	1.13	0.96	0.17
10% ZnO/AC	10	1223	850	373	1.09	0.92	0.17
CC	–	748	388	360	2.61	2.45	0.16

water bath to enable sufficient mixing of the adsorbents with the solution. Then, equilibrium concentration of DMS was measured by a high performance liquid chromatograph (HPLC, LC-10A, Shimadzu Corporation) equipped with a UV detector. To determine the concentration of DMS, the UV absorbance at 212 nm was used. The liquid-phase adsorption isotherm of DMS on AC was obtained as the relation between the equilibrium concentration and the amount of adsorbed. Furthermore, as the other impurities that are usually contained in a real bioethanol, water, acetic acid (CH₃COOH) and formic acid (HCOOH) were respectively added to ethanol, and the effect of the other impurities on the adsorption isotherms of DMS was also examined. The species and concentration of the impurities were determined based on the composition of a real bioethanol.

2.4. Packed-bed breakthrough experiment

The BTC was measured to determine the adsorption capacity of the virgin AC and the metal modified AC. 0.6 g of the adsorbent was packed in a glass column (3 mm in diameter and 300 mm in length), and a model bioethanol containing 10 ppm of DMS was introduced to the column in a flow rate of 0.2 cm³ min⁻¹. The column was kept at 293 K in an oven, and the concentration of DMS in the effluent was monitored using a photo-diode array detector. The amount of DMS adsorbed on the packed-bed was calculated using the following equation:

$$Q = \frac{F\rho_f c_0}{w} \int_0^{t_b} \left(1 - \frac{c_t}{c_0}\right) dt \quad (1)$$

where Q , F , ρ_f , c_0 , c_t , w and t_b are, respectively, the amount of DMS adsorbed on the packed bed, the flow rate of ethanol, the density of ethanol, the initial concentration of DMS, the concentration of DMS in the effluent at a certain time, the weight of adsorbent packed in the column and the breakthrough time. In this study, the breakthrough time is determined as the time when c_t/c_0 is equal to 0.05.

2.5. Numerical method for calculation of packed-bed breakthrough curve

The mass balance in the packed-bed can be expressed by the following equation:

$$\frac{\partial c}{\partial t} + V_s \frac{\partial c}{\partial z} = \frac{-(1-\varepsilon)}{\varepsilon} \frac{\partial c_s}{\partial t} + D_L \frac{\partial^2 c}{\partial z^2} \quad (2)$$

where c , c_s , t , z , V_s , ε and D_L are, respectively, the concentration of solute in the bulk phase, the concentration of solute in the particle, time, the distance along the packed bed, the superficial velocity of liquid, the void fraction of the particle and the longitudinal dispersion coefficient that can be expressed by the following equation [21]:

$$D_L = \frac{2r_s V_s}{0.20 + 0.011 R_e^{0.48}} \quad (3)$$

In the above equation, r_s denotes the radius of the particle, and R_e is the Reynolds number that is defined by the following equation:

$$R_e = \frac{2r_s V_s \rho_f}{\varepsilon \mu} \quad (4)$$

where μ is the viscosity of the bulk solution.

In Eq. (2), the concentration of the solute in the particle can be calculated by:

$$c_s = \frac{\rho_s}{(1-\varepsilon)} \bar{q} \quad (5)$$

Therefore, Eq. (2) can be expressed as:

$$\frac{\partial c}{\partial t} + V_s \frac{\partial c}{\partial z} = -\frac{\rho_s}{\varepsilon} \frac{\partial \bar{q}}{\partial t} + D_L \frac{\partial^2 c}{\partial z^2} \quad (6)$$

where ρ_s and \bar{q} denote the solid density of the particle and the mean concentration of solute in the particle, respectively. It is necessary to solve Eq. (6) with the rate equation.

In the model used in the method, adsorption of solute on an adsorbent particle is assumed to occur in the following three steps: (i) mass transfer of the solute from bulk solution to the surface of the particle; (ii) intra-particle diffusion of the solute; and (iii) adsorption of the solute to the surface of the particle. Under the assumption that step (iii) is rapid enough compared with the other two steps, the mass transfer rate from the surface to the inside of the particle can be expressed as:

$$\rho_b \frac{d\bar{q}}{dt} = ak_f(c - c_i) \quad (7)$$

where a is the surface area of the particle per unit volume of the packed bed, and k_f is the liquid-side mass-transfer coefficient that can be calculated by the following equation proposed by Wakao and Funazkri [22]:

$$k_f = \frac{(2 + 1.1S_c^{1/3} R_e^{0.6})D_{AB}}{2r_s} \quad (8)$$

where S_c is the Schmidt number as expressed by Eq. (9):

$$S_c = \frac{\mu}{\rho_f D_{AB}} \quad (9)$$

In the above equations (8) and (9), D_{AB} is bulk diffusivity of solute and can be estimated using the following equations (10) and (11) [23]:

$$D_{AB} = \frac{KT}{\mu V_A^{1/3}} \quad (10)$$

$$K = (8.2 \times 10^{-8}) \left[1 + \left(\frac{3V_B}{V_A} \right)^{2/3} \right] \quad (11)$$

where T , V_A and V_B are temperature, the molar volume of solute and solvent, respectively.

On the other hand, the mass transfer rate of solute from the surface to the inside of the particle per unit volume is

$$\rho_b \frac{d\bar{q}}{dt} = -aD_s \rho_b \left. \frac{\partial q}{\partial r} \right|_{r=r_s} \quad (12)$$

where D_s and ρ_b are, respectively, the effective diffusivity of solute in the particle and the bulk density of the particle. Using the linear driving force approximation, the diffusion rate of solute inside the particle can be expressed as follows:

$$\rho_b \frac{d\bar{q}}{dt} = \frac{5aD_s \rho_s}{r_s} (q_i - \bar{q}) \quad (13)$$

where q_i is the concentration of the solute on the surface of the particle. In this study, q_i is determined by analyzing the adsorption isotherm based on the Freundlich-type adsorption model, that accounts for multilayer sorption on heterogeneous surfaces in a liquid phase as expressed by the following equation:

$$q_i = K_F c_i^{1/n} \quad (14)$$

where c_i is the equilibrium concentration of solute in a liquid phase. K_F and n are the Freundlich constants, and n corresponds to the heterogeneity of the adsorption sites [24,25]. We use the Freundlich model to analyze the experimental data, since activated carbon generally gives isotherms that obey the Freundlich equation except for the high concentration range. Eq. (15) is the linearized form of

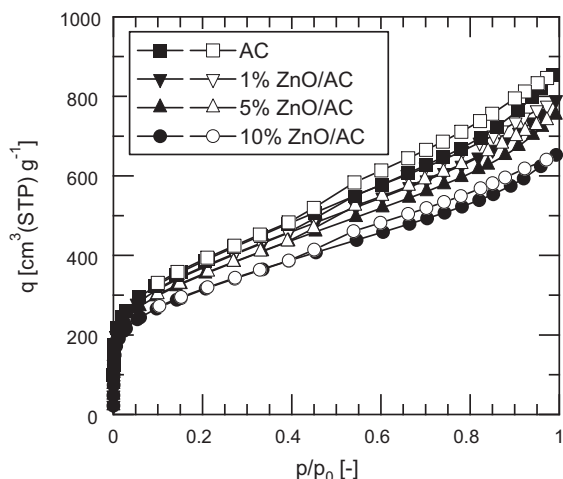


Fig. 1. Isotherms of nitrogen on activated carbon at 77 K; closed symbols: adsorption branch, open symbols: desorption branch.

Eq. (14). The slope of the line gives the value of $1/n$ and the intercept of the line gives the value of $\log K_F$:

$$\log q_i = \log K_F + \frac{1}{n} \log c_i \quad (15)$$

Thus determined Freundlich parameters are used to calculate a BTC based on a numerical method.

Based on the equations from (2) to (15), the column equation is solved by the numerical method of lines using the differential equation solver (LSODES) [26]. LSODES is a Livermore solver variant that can solve the initial value problem as first-order partial differential equations with general sparse Jacobian matrices. Each time step, the concentration on the surface of the particle is iteratively calculated for one variable minimization. As a result, a BTC curve for the packed-bed can be calculated as the plot of concentration versus time in the end of the column. (Flow chart of the numerical method is depicted in supporting information S2.)

3. Results and discussion

3.1. Porous properties of activated carbon

Fig. 1 shows the effect of the loading ratio of zinc oxide on the isotherms of nitrogen. The porous properties of the adsorbents employed in this study are summarized in Table 1. If the loading ratio of metal oxide is as small as 1.0 wt.%, the porous structure of the metal-loaded AC is almost the same as that of the virgin AC. It is evident that the volume of mesopores of the AC loaded with zinc oxide, V_{mes} , decreases with increasing the loaded ratio from 1.0 to 10.0 wt.%, indicating that zinc oxide is mainly loaded on the mesopores of AC rather than the micropores.

3.2. Adsorption characteristics of activated carbon in batch system

Fig. 2 shows the transient change in concentration of DMS in ethanol when the adsorbent (AC) is added. The gradual decrease in the concentration of DMS continues for about 24 h. Based on the result, all adsorption isotherms of DMS were measured at the equilibrium time of 24 h.

Fig. 3 shows the adsorption isotherms of DMS on AC loaded with different amounts of zinc oxide. As depicted in Fig. 3 with a solid line, the adsorption isotherms can be fitted by the isotherm based on the Freundlich model. The Freundlich parameters estimated by

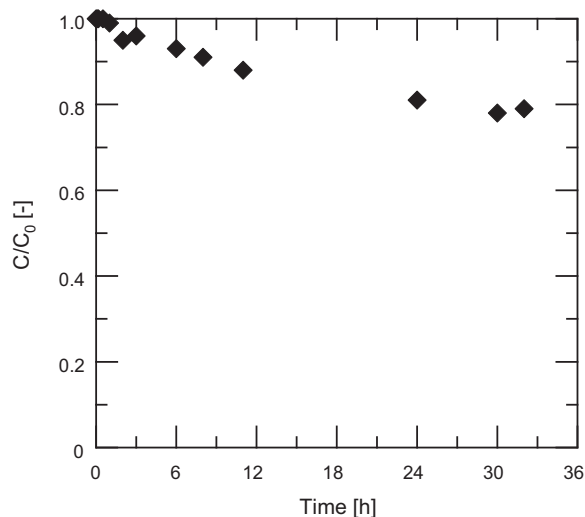


Fig. 2. Transient change in concentration of DMS in ethanol containing AC at 293 K; 0.1 g of adsorbents was added to 40 cm³ of ethanol, $C_0 = 10$ ppm.

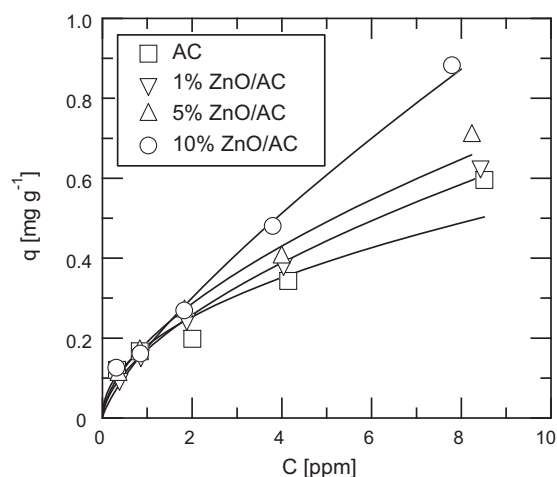


Fig. 3. Liquid-phase adsorption isotherm of DMS in ethanol, solid line: fitted curve by the Freundlich model, adsorbent: AC loaded with different amounts of zinc oxide.

applying Eq. (14) to the measured isotherms are summarized in Table 2. As shown in Fig. 3, it is noteworthy that the amount of DMS adsorbed on AC clearly increased with increasing the loading ratio of zinc oxide. Similar to the previous result reported by Cui and Turn [14] on the gas-phase adsorptive desulfurization using metal-modified activated carbon, this result shows that the adsorption capacity of the AC in a liquid phase can be increased by the Lewis acid/base interaction between DMS and zinc oxide loaded on AC.

Fig. 4 shows the adsorption isotherms of DMS on AC in the presence of the other impurities. It is noteworthy that the isotherms of DMS in the presence of the other impurities are almost unchanged

Table 2
Freundlich parameters of liquid-phase adsorption of DMS.

Adsorbent	Freundlich parameter		r^2
	$1/n$	K_F [mg g ⁻¹ ppm ^(-1/n)]	
AC	0.47	0.18	0.95
1% ZnO/AC	0.60	0.17	0.99
5% ZnO/AC	0.59	0.19	0.99
10% ZnO/AC	0.62	0.21	0.96

r^2 : correlation coefficient in the fitting by the Freundlich equation.

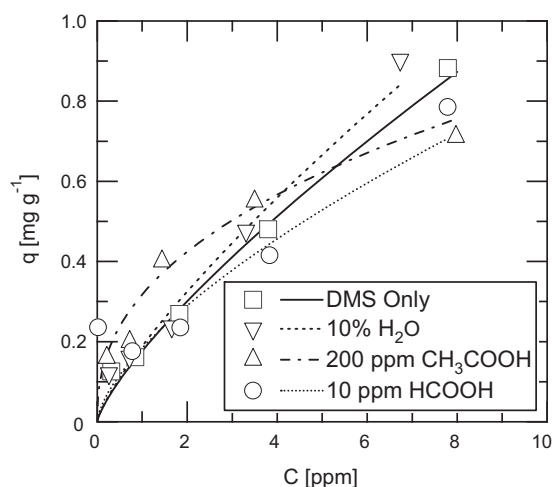


Fig. 4. Effect of other impurities on liquid-phase adsorption isotherm of DMS in ethanol; line: fitted curve by the Freundlich model, adsorbent: 10% ZnO/AC.

from that measured in the absence of the other impurities. Thus, we concluded that the prepared adsorbent was applicable to adsorptive desulfurization of a real bioethanol that contained the other impurities.

3.3. Adsorption characteristics of activated carbon in packed bed

Fig. 5 shows a BTC measured by using an adsorption column packed with 10% ZnO/AC. The amount of DMS that can be removed by the packed bed is calculated from the breakthrough time (approximately at 5 min) as 0.22 mg g^{-1} . This amount might be smaller than the adsorbed amount expected from the adsorbed isotherms shown in Fig. 3. This is because diffusivity of DMS in the micropores of AC is small as can be assumed from Fig. 2. By using the process parameters listed in Table 3, the calculated BTCs are also shown in Fig. 5. The effective diffusivity of DMS in solid (D_s) and superficial velocity of liquid (V_s) are, respectively, varied to coincide a calculated BTC with the measured one. As a result of the fitting, D_s and V_s are determined as $1.8 \times 10^{-11} \text{ m}^2 \text{ s}^{-1}$ and $8.0 \times 10^{-3} \text{ m s}^{-1}$, respectively.

According to the result of our preliminary study, concentration of DMS contained in bioethanol is found to be in the range of 0.1–10 ppm. To design a packed-bed for desulfurization of bioethanol, as shown in Fig. 6, a BTC under the different initial concentrations (0.1 ppm or 1 ppm) of DMS is calculated using the above determined values of D_s and V_s . (In the calculation, only c_0 is changed.) For example, when the initial concentration of DMS is 0.1 ppm, the breakthrough time can be predicted to be 30 min. This implies that $1.0 \times 10^{-2} \text{ m}^3$ of bioethanol that contains 0.1 ppm of

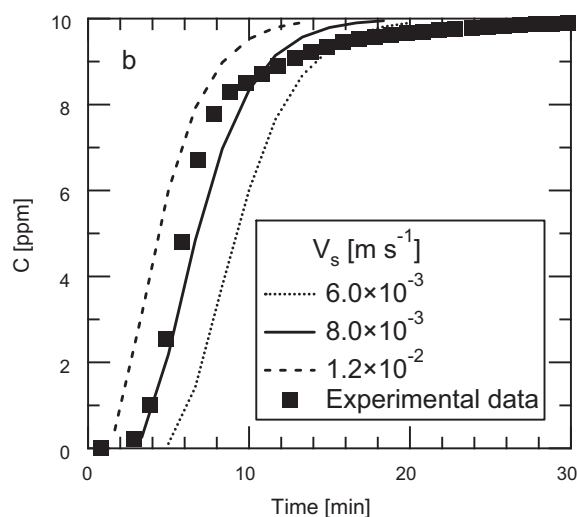
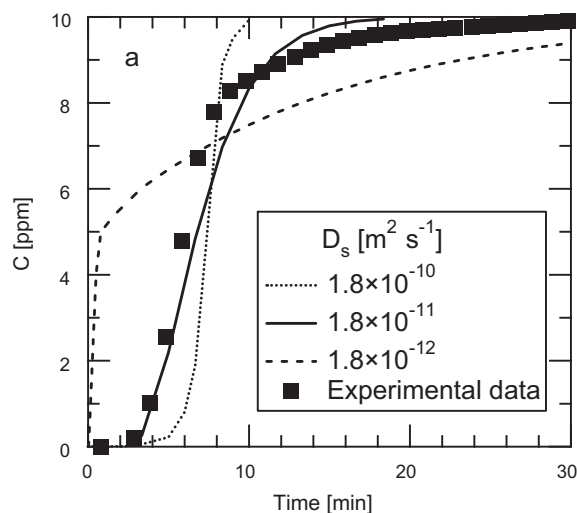


Fig. 5. Calculated and measured breakthrough curves of DMS in ethanol; adsorbent: 10% ZnO/AC.

Table 3

Parameters used for calculation of a packed-bed breakthrough curve of DMS in ethanol.

Parameter	
Diameter of particle, $2r_s$ [m]	1.9×10^{-4}
Length of bed, z [m]	3.0×10^{-1}
Feed concentration, c_0 [ppm]	1.0×10^1
Bulk density of bed, ρ_b [kg m^{-3}]	2.8×10^2
Diffusivity in fluid, D_{AB} [$\text{m}^2 \text{ s}^{-1}$]	1.5×10^{-9}
Fluid viscosity, μ [Pa s]	8.6×10^{-4}
Fluid density, ρ_f [kg m^{-3}]	7.9×10^2
Void fraction of bed, ε	5.5×10^{-1}
Freundlich parameters	
K_F [$\text{mg g}^{-1} \text{ ppm}^{(-1/n)}$]	2.1×10^{-1}
$1/n$	6.7×10^{-1}

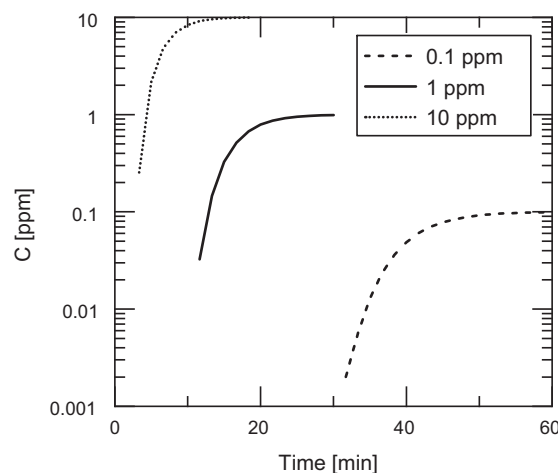


Fig. 6. Calculated breakthrough curves of DMS in ethanol under different initial concentrations; adsorbent: 10% ZnO/AC, parameters determined by the fitting ($D_s = 1.8 \times 10^{-11} \text{ m}^2 \text{ s}^{-1}$, $V_s = 8.0 \times 10^{-3} \text{ m s}^{-1}$) are used.

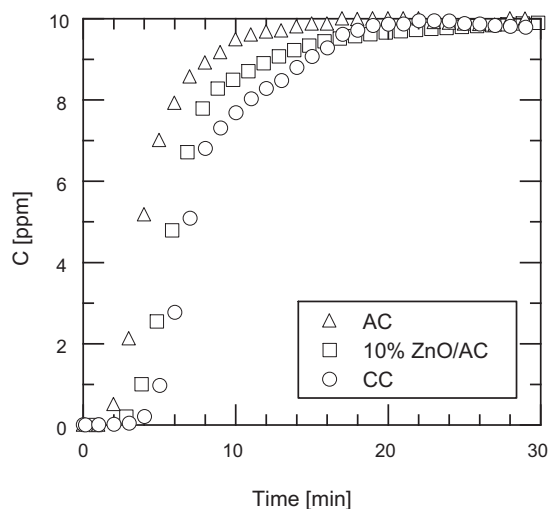


Fig. 7. Breakthrough curves of DMS in ethanol measured by using adsorbents with different pore size distributions.

DMS can be desulfurized using a column packed with 1 kg of 10% ZnO/AC.

Fig. 7 shows the BTC measured by using CC with larger pore sizes than AC. The pore size distributions of the adsorbents are shown in Fig. 8. The breakthrough time was found to increase in the order of $AC < 10\% ZnO/AC < CC$. Although AC and 10% ZnO/AC possess almost the same pore size distribution, the breakthrough time in the case of using 10% ZnO/AC is longer than that of using AC. It may be explained with the Lewis acid/base interaction between DMS and zinc oxide as discussed in the previous section. It should be noted that CC possessing the largest pore size among the employed adsorbents shows the largest adsorption capacity for DMS. The measured and calculated BTCs using CC are shown in Fig. 9. As the result of the calculation of a BTC to coincide with the measured one, D_s and V_s were determined as $1.8 \times 10^{-10} \text{ m}^2 \text{ s}^{-1}$ and $1.8 \times 10^{-2} \text{ m s}^{-1}$, respectively. Although the solid diffusivity of DMS in the CC particles is smaller than the value of $1.5 \times 10^{-9} \text{ m}^2 \text{ s}^{-1}$ in a bulk phase [23], it is significantly larger than that in the AC particles. This indicates that the removal efficiency of DMS can be further increased by using the adsorbent that possesses larger mesopores.

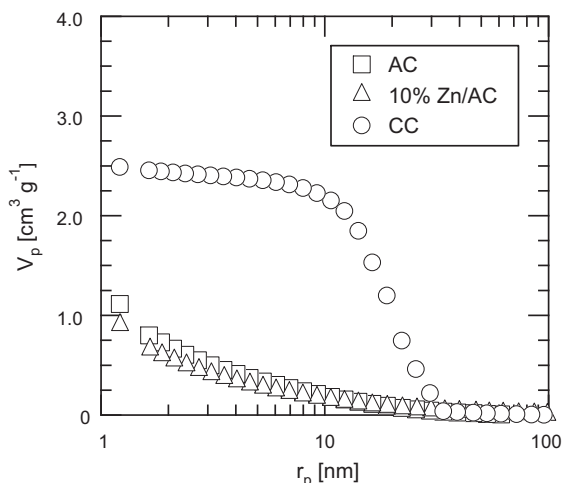


Fig. 8. Pore size distributions of adsorbents.

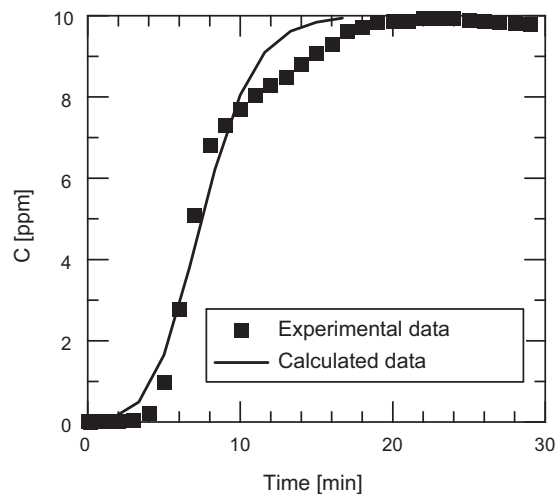


Fig. 9. Calculated and measured breakthrough curves of DMS in ethanol; adsorbent: CC, parameters determined by the fitting ($D_s = 1.8 \times 10^{-10} \text{ m}^2 \text{ s}^{-1}$, $V_s = 1.8 \times 10^{-2} \text{ m s}^{-1}$) are used.

4. Conclusions

Bioethanol contains a sulfur impurity such as DMS that influences on the ETO reaction. In the present study, to develop a liquid-phase adsorptive desulfurization process of bioethanol, the effect of metal modification of activated carbon on the adsorption performance to remove DMS from a model bioethanol was studied. Consequently, we confirmed that the amount of DMS adsorbed on activated carbon loaded with 10 wt.% of zinc oxide was twice as much as that on virgin activated carbon. It was also revealed that the adsorption performance of the activated carbon in the model bioethanol was almost unchanged by the presence of the other impurities, such as water, acetic acid and formic acid. By measuring a BTC of DMS in ethanol using a column packed with the prepared adsorbents, the mass-transfer parameters necessary for designing the liquid-phase adsorptive desulfurization process were estimated based on the numerical method. As a result, a BTC under the different initial concentrations of DMS could also be calculated. To further improve the performance of the adsorptive desulfurization process, use of activated carbon with larger mesopores is considered to be effective, which will be examined in our subsequent study.

Acknowledgements

The authors are grateful to the financial support from the New Energy and Industrial Technology Development Organization (NEDO). The authors are thankful to Dr. N. Ikawa for his assistance and suggestion in XRD measurement.

Appendix A. Supplementary data

Supplementary data associated with this article can be found, in the online version, at doi:10.1016/j.cej.2010.09.020.

References

- [1] Y.I. Makarfi, M.S. Yakimova, A.S. Lermontov, V.I. Erofeev, L.M. Koval, V.F. Tretiyakov, Conversion of bioethanol over zeolites, Chem. Eng. J. 154 (2009) 396–400.
- [2] G. Chen, S. Li, F. Jiao, Q. Yuan, Catalytic dehydration of bioethanol to ethylene over $TiO_2/\gamma-Al_2O_3$ catalysts in microchannel reactor, Catal. Today 125 (2007) 111–119.

- [3] A.L. Valant, A. Garron, N. Bion, F. Epron, D. Duprez, Hydrogen production from raw bioethanol over Rh/MgAl₂O₄ catalyst: impact of impurities: heavy alcohol, aldehyde, ester, acid and amine, *Catal. Today* 138 (2008) 169–174.
- [4] S. Kakui, N. Shimotsuma, T. Kyotani, K. Sawamura, K. Yamaguchi, S. Ikeda, T. Nakane, Remarkable emission intensity of dimethyl sulfide from-sulfur on the determination of sulfur in biomass ethanol by inductively coupled plasma-optical emission spectrometry, *Bunseki Kagaku* 56 (2007) 587–591.
- [5] S. Landaud, S. Helinck, P. Bonnarme, Formation of volatile sulfur compounds and metabolism of methionine and other sulfur compounds in fermented food, *Appl. Microbiol. Biotechnol.* 77 (2008) 1191–1205.
- [6] K. Yokota, K. Fujimoto, Effects of sulfur-containing compounds on methanol conversion over ZSM-5 catalyst, *Nihonkagaku* 3 (1989) 601–603.
- [7] M. Katoh, T. Yamazaki, N. Kikuchi, Y. Okada, T. Yoshikawa, M. Wada, Conversion of bio-ethanol into hydrocarbons over HZSM-5 catalyst, *Kagaku Kogaku Ronbunshu* 34 (2008) 396–401.
- [8] I.V. Babich, J.A. Moulijn, Science and technology of novel processes for deep desulfurization of oil refinery streams: a review, *Fuel* 82 (2003) 607–631.
- [9] S. Haji, C. Erkey, Removal of dibenzothiophene from model diesel by adsorption on carbon aerogels for fuel cell applications, *Ind. Eng. Chem. Res.* 42 (2003) 6933–6937.
- [10] C. Laborde-Boutet, G. Joly, A. Nicolaos, M. Thomas, P. Magnoux, Selectivity of thiophene/toluene competitive adsorptions onto NaY and NaX zeolites, *Ind. Eng. Chem. Res.* 45 (2006) 6758–6764.
- [11] M.A. Al-Ghoutia, Y.S. Al-Degsb, F. Khalili, Minimisation of organosulphur compounds by activated carbon from commercial diesel fuel: mechanistic study, *Chem. Eng. J.* 162 (2010) 669–676.
- [12] H. Wakita, Y. Tachibana, M. Hosaka, Removal of dimethyl sulfide and *t*-butylmercaptan from city gas by adsorption on zeolites, *Micropor. Mesopor. Mater.* 46 (2001) 237–247.
- [13] D. Crespo, G. Qi, Y. Wang, F.H. Yang, R.T. Yang, Superior sorbent for natural gas desulfurization, *Ind. Eng. Chem. Res.* 47 (2008) 1238–1244.
- [14] H. Cui, S.Q. Turn, Adsorption/desorption of dimethylsulfide on activated carbon modified with iron chloride, *Appl. Catal. B: Environ.* 88 (2009) 25–31.
- [15] H. Cui, S.Q. Turn, M.A. Reese, Removal of sulfur compound from utility pipelined synthetic natural gas using modified activated carbons, *Catal. Today* 139 (2009) 274–279.
- [16] I. Rosso, C. Galletti, M. Bizzi, G. Saracco, V. Specchia, Zinc oxide sorbents for the removal of hydrogen sulfide from syngas, *Ind. Eng. Chem. Res.* 42 (2003) 1688–1697.
- [17] X. Wang, T. Sun, J. Yang, L. Zhao, J. Jia, Low-temperature H₂S removal from gas stream with SBA-15 supported ZnO nanoparticles, *Chem. Eng. J.* 142 (2008) 48–55.
- [18] T. Yamamoto, A. Endo, T. Ohmori, M. Nakaiwa, The effects of different synthetic conditions on the porous properties of carbon cryogel microspheres, *Carbon* 43 (2005) 1231–1238.
- [19] G. Carlson, D. Lewis, K. McKinley, J. Richardson, T. Tillotson, Aerogel commercialization: technology, markets and costs, *J. Non-Cryst. Solids* 186 (1995) 372–379.
- [20] F. Rouquerol, J. Rouquerol, K. Sing, Assessment of surface area (Chapter 6), in: *Adsorption by Powders & Porous Solids*, Academic Press, San Diego, 1999, pp. 165–183.
- [21] S. Chung, C. Wen, Longitudinal dispersion of liquid flowing through fixed and fluidized beds, *AIChE J.* 14 (1968) 857–866.
- [22] N. Wakao, T. Funazkri, Effect of fluid dispersion coefficients on particle-to-fluid mass transfer coefficients in packed bed, *Chem. Eng. Sci.* 33 (1978) 1375–1384.
- [23] R.H. Perry, D.W. Green, *Perry's Chemical Engineering Handbook*, sixth ed., McGraw-Hill Book Company, New York, 1973.
- [24] L.J. Kennedy, J.J. Vijaya, K. Kayalvizhi, G. Sekaran, Adsorption of phenol from aqueous solutions using mesoporous carbon prepared by two-stage process, *Chem. Eng. J.* 132 (2007) 279–287.
- [25] V. Fierro, V. Torné-Fernández, D. Montané, A. Celzard, Adsorption of phenol onto activated carbons having different textural and surface properties, *Micropor. Mesopor. Mater.* 111 (2008) 276–284.
- [26] W.E. Schiesser, *The Numerical Method of Lines: Integration of Partial Differential Equations*, Academic Press, San Diego, 1991.